Supplementary Material for "Cell responses only partially shape cell-to-cell variations in protein abundances in *Escherichia coli* chemotaxis."

I. Models of E. coli chemotaxis: We studied three different coarse-grained or approximate models that were proposed to explain E. coli chemotaxis: (i) the modified BL (MBL) model (1), which is a recently proposed modification of the BL model (2), (ii) the Barkai-Leibler (BL) model (2), and (iii) the fine-tuned (FT) model (3, 4). The biochemical reactions describing the models are shown in Fig. S1. Each model is composed of a set of biochemical reactions involving the chemotactic proteins, CheA, CheR, CheB, CheY, CheZ (not considered in the BL model), and the transmembrane Tar receptors. The models also differ from each other due to differences in their molecular wiring (Fig. S1). We provide details regarding each model below. The average abundances of the proteins in all the three models are shown in Table S1A. The activation probabilities for the receptors are shown in Table S1B.

(i) *MBL model:* Sourjik and colleagues proposed and experimentally tested a modified version of the BL model (MBL, Fig. S1C) that was able to restrain variations in the steady state of CheY-P concentration to a small range (1). The biochemical reactions and the rates used are given in Table S2A.

(ii) *FT model:* The FT model (Fig. S1A) was among the first proposed models that could explain precise adaptation in *E. coli* only within a narrow range of rate constants and protein concentrations (3, 4). We constructed the FT model by adding an extra module to the MBL model where the CheB-P can de-methylate the inactive forms of the Tar receptor complex (Tar_m as opposed to Tar_m^A) as well. The reactions and the parameters used in the model are shown in Table S2B. Our version of the FT model, though very similar in essence to the original Knox et al. (4) and Hauri and Ross (3) model, harbors a few differences worth mentioning. Hauri and Ross approximated the Tar, CheW and CheA into one complex, which they referred to as T. They did not consider an explicit auto phosphorylation of CheA. We have an explicit auto phosphorylation reaction of CheA with a rate proportional to the total number of active Tar complex. Unlike Hauri and Ross model, CheA, instead of the complex T, transfers the phosphate group to CheY and CheB. We have explicitly considered the phosphatase CheZ. Hauri and Ross assumed a first order de-activation of CheY-P.

(iii) *BL model*: The BL model (Fig. S1B) was able to capture the robustness of the nearly perfect nature of adaptation of *E. coli* chemotaxis to variations in rate constants or strengths of protein-protein interactions (2), as confirmed in cell population experiments (5). However, the steady state concentration of phosphorylated CheY protein (or CheY-P) in the BL model is sensitive to large variations of protein concentrations in the model.

Since the working range of the flagella motor is limited to small variations (~30%) from the optimal CheY-P concentration, the robustness of *E. coli* adaptation to large range of variation in the abundance of chemotactic proteins requires small variations of steady state CheY-P concentrations(1, 6). The biochemical reactions and the rates used are given in Table S2C.

II. In silico simulations of E. coli chemotaxis: We used a rule based software package BIONETGEN(7) to simulate the deterministic and stochastic kinetics described by the biochemical reactions associated with each model. The signaling molecules are assumed to be well mixed in the simulation box representing a single E. coli cell.

(A) Evaluation of the pre-stimulus state: All the simulations were initialized at $t^{initial}$ = -800000 s with protein abundances, $Tar_{m=0}(t^{initial}) = Tar^T$, $CheA(t^{initial}) = CheA^T$, $CheR(t^{initial}) = CheR^T$, $CheB(t^{initial}) = CheB^T$, $CheY(t^{initial}) = CheY^T$ and $CheZ(t^{initial}) = CheZ^T$ while abundances of all other species (methylated receptors ($m \neq 0$) and phosphorylated form of all the other proteins) are set to zero. The superscript T refers to total abundances of the respective proteins in a single *E. coli* cell. We solve the ODEs describing the deterministic chemotactic kinetics to obtain steady state values of the protein abundances. The steady state values of the abundances define the pre-stimulus state of the chemotactic kinetics. The ODEs, instead of the stochastic kinetics, were used to make the calculations computationally efficient because the contributions of the intrinsic noise fluctuations to the steady state values of the ODEs were small (Supplementary Figure 4 in Mukherjee et al. (8)). The BIONETGEN files for the simulations are available at http://planetx.nationwidechildrens.org/~jayajit/Ecoli_chemotaxis_bionetgen_codes/.

(B) Simulation of the chemotactic response: The steady state protein abundances in the pre-stimulus state are used as initial conditions. The attractants (100μM of L-aspartate) are added in the system at $t=t_0=0$. We do not consider explicit ligand receptor interaction. The effect of ligand binding is subsumed in the probabilities a(L) of the methylated receptors to be in an active state (Table S1B). The stochastic simulations solve the Master Equation associated with the biochemical reactions exactly following the Gillespie method. The adaptation time (τ_Γ), variation in the steady state CheY-P abundance (p_Γ), and the precision of adaptation (s_Γ) are calculated for each stochastic trajectory Γ representing the chemotactic response in an individual cell. The stochastic simulations are carried out until t =2000s which is much larger than the typical adaptation time for E.coli for a 100μM L-aspartate stimulation. When the CheY-P abundance in an individual cell does not recover to the half of the pre-stimulus steady state CheY-P abundance within 2000 s, we assign a very large number (6×10^6 s) to τ to mark the cell that did not adapt in a realistic time scale. The pre-stimulus steady state abundance of CheY-P ([CheY-P]) varies from cell to cell due to the variations of total protein

abundances in individual *E. coli* cells. The variation of the steady state abundance of CheY-P needs to be within 30% from an optimal value for proper functioning of the flagellar motor (1, 6). We calculate the variation of steady state CheY-P abundance (p) in single *E. coli* cells using the equation below, $\mathrm{p} = \left| \frac{[\mathrm{CheY-P}]_{\mathrm{pre-stim}} - [\mathrm{CheY-P}]_{\mathrm{optimal}}}{[\mathrm{CheY-P}]_{\mathrm{optimal}}} \right|$.

Optimal value of CheY-P ($[\text{CheY-P}]_{\text{optimal}}$), is defined as the ODE based solution of the steady state value of the CheY-P when the total protein concentrations are set to the values quoted in Li et al (9). We calculate $[\text{CheY-P}]_{\text{pre-stim}}$ using the ODE solutions ignoring intrinsic noise fluctuations for the reasons mentioned above.

III. Evaluation of the distributions corresponding to the MaxEnt state. MaxEnt provides a powerful tool to address such questions that require inference of model parameters based on available experimental data. The concept of the Maximum Entropy (MaxEnt) principle was seeded in the second law of thermodynamics which states that the entropy of an isolated system in equilibrium never decreases(10). The use of MaxEnt to infer distribution functions without imposition of any additional assumptions was pioneered by E. T. Jaynes and others (11, 12) where the Shannon's entropy (S) is maximized subject to constraints imposed by experimental data. These methods have been widely used in diverse disciplines including physics(10), information theory(13), econometrics, and, biology (14-17) to estimate probability distributions that are consistent with available experimental data (14, 16-18). We use an extension of the MaxEnt based approaches where Shannon's entropy constructed from distributions of temporal profiles of abundances of chemotactic signaling proteins is maximized. This method is known as the Maximum Caliber (MaxCal), also proposed by Jaynes to extend the MaxEnt approach to dynamical systems(12, 18, 19).

(A) Derivation of the inferred distribution $\hat{P}(\{n_q^{\text{total}}\})$ when the chemotactic responses are constrained

We describe our method of inferring distributions of total abundances of protein species in individual E. coli cells below. We define the Shannon's entropy for the stochastic trajectories $\{\Gamma\}$ as,

$$S = -\sum_{\Gamma} P_{\Gamma} \ln P_{\Gamma} \qquad \text{(S1)}$$

When attractants are added at time $t=t_0$, the stochastic trajectory, Γ, represents changes in the abundances of signaling proteins in an individual cell in a time interval t_0 to t_n by a set $(\{n_j\}, t_n ; \{n_j\}, t_{n-1} ; \{n_j\}, t_{n-2} ;\ldots; \{n_j\}, t_1;\{n_j\}, t_0; \{n^{\text{total}}{}_q\})$ where copy numbers of

different proteins, $\{n_j\}$ (j=1…N_P = total # of distinct signaling proteins), are given at times, $t_{n-i} = t_0 + (n-i)\Delta$, i=0..n, where, Δ is smaller than or of the same order as the smallest reaction time scale (Fig. 2). q denotes the number of different protein species, N_T. $N_P \geq N_T$, as a protein species can be modified during signaling, e.g., the signaling protein CheY-P is generated from the protein CheY.

Therefore,

$$\begin{aligned} P_\Gamma &= P(\{n_j\},t_n;\{n_j\},t_{n-1};\{n_j\},t_{n-2};\cdots|\{n_j\},t_0)P(\{n_j\},t_0;\{n_q^{total}\}) \\ &= P(\{n_j\},t_n;\{n_j\},t_{n-1};\{n_j\},t_{n-2};\cdots|\{n_j\},t_0)P(\{n_j\},t_0|\{n_q^{total}\})P(\{n_q^{total}\}) \end{aligned} \quad \text{(S2)}$$

$P(\{n_j\}, t_n ; \{n_j\}, t_{n-1} ; \{n_j\}, t_{n-2} ;\ldots; \{n_j\}, t_1 \mid \{n_j\}, t_0)$ is the conditional probability of producing the copy numbers of the signaling species in a stochastic trajectory Γ at the times $\{t_n \ldots t_1\}$, given there is a specific set of copy numbers of proteins ($\{n_j\}$) when attractants are added at the pre-stimulus state at t_0. $P(\{n_j\}, t_0; \{n^{total}_q\})$ denotes the joint probability of having the pre-stimulus state with specific copy numbers ($\{n_j\}$) at time t_0 and total protein concentrations $\{n^{total}_q\}$. This joint probability can be written as a product of the conditional probability $P(\{n_j\}, t_0 | \{n^{total}_q\})$, describing the probability for having the pre-stimulus state at t_0 given a specific set of total protein abundances $\{n^{total}_q\}$, and the probability of occurrence of $\{n^{total}_q\}$ or $P(\{n^{total}_q\})$, i.e, $P(\{n_j\}, t_0; \{n^{total}_q\}) = P(\{n_j\}, t_0 | \{n^{total}_q\}) P(\{n^{total}_q\})$.

The biochemical signaling reactions producing E. coli chemotaxis are described by Markov processes where the conditional probability, $P(\{n_j\}, t_p | \{n_j\}, t_{p-1})$, for changing the signaling state of the system changes from $\{\{n_j\}, t_{p-1}\}$ to $\{\{n_j\}, t_p\}$ is given by the Master Equation(20),

$$\partial P(\{n_j\};t_p|\{n_j\};t_{p-1})/\partial t_p = L\,P(\{n_j\};t_p|\{n_j\};t_{p-1}) \quad \text{(S3)}$$

, where, L describes a linear operator (20) dependent on the biochemical reaction rates, wiring of the signaling network in a signaling model (e.g., MBL), and the copy numbers of signaling proteins at time t_{p-1}. Therefore, the conditional probability, $P(\{n_j\}, t_n ; \{n_j\}, t_{n-1} ; \{n_j\}, t_{n-2} ;\ldots; \{n_j\}, t_1 \mid \{n_j\}, t_0) = P(\{n_j\}, t_n \mid \{n_j\}, t_{n-1}) P(\{n_j\}, t_{n-1} \mid \{n_j\}, t_{n-2}) \ldots P(\{n_j\}, t_1 \mid \{n_j\}, t_0)$ (equality holds for a Markov process), is entirely determined by the solutions of the above Master Equation and the initial condition at $t=t_0$. We consider variations in P_Γ arising from the variations in $P(\{n^{total}_q\})$, i.e.,

$$\delta P_\Gamma = P(\{n_j\},t_n;\{n_j\},t_{n-1};\{n_j\},t_{n-2};\cdots|\{n_j\},t_0)P(\{n_j\},t_0|\{n_q^{total}\})\delta P(\{n_q^{total}\}) = P_C\,\delta P(\{n_q^{total}\}) \quad \text{(S4)}$$

where, we define

$$P_C = P(\{n_j\},t_n;\{n_j\},t_{n-1};\{n_j\},t_{n-2};\cdots|\{n_j\},t_0)P(\{n_j\},t_0|\{n_q^{total}\})$$
$$= P(\{n_j\},t_n;\{n_j\},t_{n-1};\{n_j\},t_{n-2};\cdots;\{n_j\},t_0|\{n_q^{total}\})$$

to simplify notations.

We maximize S in Eq. (S1) when the total protein abundances are varied as above in the presence of the constraint given by Eq. (S5) below.

When a variable, f_Γ, describes a chemotactic response (such as τ) that depends on the stochastic trajectory Γ produced in a single E. coli cell indexed by α, the cell population averaged value of f_Γ is given by:

$$\frac{1}{\text{total \# of cells}}\sum_{\alpha=1}^{\text{total \# of cells}} f_\alpha = \sum_\Gamma f_\Gamma P_\Gamma = \overline{f}^{\text{expt}} \qquad \text{(S5)}$$

When $P_\Gamma = \hat{P}_\Gamma$ or $P(\{n_q^{total}\}) = \hat{P}(\{n_q^{total}\})$ maximizes the entropy S in Eq. (S1), small variations of P_Γ as in Eq. (S4) around $P_\Gamma = \hat{P}_\Gamma$, i.e., $P_\Gamma = \hat{P}_\Gamma + \delta P_\Gamma$, will produce the equation below. For simplifying the notation we abbreviate, $P(\{n_q^{total}\})$ as P_0.

$$\delta S = 0 = \sum_\Gamma P_C(\ln P_C + \ln P_0)(\delta P_0) + \sum_\Gamma P_C(\delta P_0) \qquad \text{(S6)}$$

The same variations in P_Γ will yield the equation below from the constraint equation, Eq. (S5),

$$0 = \sum_\Gamma f_\Gamma P_C(\delta P_0) \qquad \text{(S7)}$$

Therefore by solving for $\hat{P}(\{n_q^{total}\})$ using Eq. (S6) and Eq. (S7),

$$\hat{P}(\{n_q^{total}\}) = Z^{-1}Q_C \exp(-\lambda\sum_{\Gamma_C} f_\Gamma P_C) \qquad \text{(S8)}$$

where, $\ln Q_C = -\sum_{\Gamma_C} P_C \ln P_C$ and Γ_C describes the stochastic trajectory ($\{n_j\}$, t_n ; $\{n_j\}$, t_{n-1} ; $\{n_j\}$, t_{n-2} ;…; $\{n_j\}$, t_1;$\{n_j\}$, t_0) with a fixed specific total protein abundances, $\{n_q^{total}\}$. Therefore, summation over Γ_C essentially denotes averages over variations of stochastic trajectories due to intrinsic noise fluctuations. λ is the Lagrange multipliers, which is determined by substituting Eq. (S8) in constraint equation (Eq. (S5)). Z is the partition function. In deriving Eq. (S8), we also used the fact, $\sum_{\Gamma_C} P_C = 1$. Eq. (S8) can be easily generalized to include additional constraints describing average values and higher order moments of variables (such as τ, s, and p) describing chemotactic responses in single E.

coli cells. The conditional probability, P_C, and thus Q_C, in principle, can be calculated by solving the Master Eq. (S3) for the E. coli chemotaxis signaling models (MBL, BL or FT) we considered. We used an approximate numerical scheme to evaluate Q_C in our simulations (see section B). However, in general, it is possible that the underlying biochemical reactions in a model are not known and consequently P_C cannot be evaluated by solving the Master Equation in Eq. (S3). In similar situations, when it is possible to do repeated experiments, constraints on $\ln Q_C$ have been imposed to infer parameter distributions(21-23). Though we do not face this issue for the models in E. coli chemotaxis where the signaling reactions are very well characterized, the same formalism developed above can be used in signaling systems where the intrinsic noise fluctuations are not well characterized. In such cases, the distribution of total protein abundances can be evaluated by extending Eq. (S8) with additional Lagrange multipliers incorporating constraints for $\ln Q_C$. However, imposition of constraints on $\ln Q_C$ would require data available from repeated experiments probing signaling kinetics on the same individual cell or when independent signaling modules exist in the same cell which can be assayed simultaneously(24).

(B) *Calculation of* $\hat{P}(\{n_q^{\text{total}}\})$ *in simulations when the chemotactic responses are constrained*

We first create *a priori* distribution of the protein abundances by choosing total protein abundances at t^{initial} = -800000 s from a uniform distribution U(0, U_H), where U_H is chosen to be roughly 10 times larger than the experimentally measured mean abundance of the corresponding chemotactic protein (9). This step essentially creates a cell population where an individual cell is assigned with a set of total protein abundances chosen randomly from the above uniform distribution. We used up to 70,000 samples (or cells) drawn from the above uniform distribution. Then following the procedure described in section (II) we simulate the chemotactic signaling kinetics in individual cells. In the samples we used in our simulations, each *E. coli* cell produces a unique chemotactic response kinetics or a stochastic trajectory describing time evolution of abundances of signaling proteins, therefore we identify each trajectory by the single cell that generated it and vice versa. Thus the simulations generate a set of stochastic trajectories $\{\Gamma\}$ uniquely associated with a set of single cells. From this set of stochastic trajectories,$\{\Gamma\}$, we evaluated the distribution in Eq. (4). The summation over Γ_C is carried out by using the unique association of a stochastic trajectory with a single cell in our simulations as this implies that for a particular stochastic trajectory, $\Gamma'_C = \{\{n'_j\}, t_n ; \{n'_j\}, t_{n-1} ; \ldots; \{n'_j\}, t_0\}$ associated with a fixed set of total protein concentrations $\{ n'^{\text{total}}_q\}$, $P_C = P(\{n'_j\}, t_n ; \{n'_j\}, t_{n-1} ; \ldots; \{n'_j\}, t_0 \mid \{n'^{\text{total}}_q\})$ is either equal to 1 (when Γ'_C

or the corresponding single cell is present in the samples we considered) or 0 (when Γ'_C is absent in the samples). Thus, $\sum_{\Gamma_C} P_C \ln P_C = 0$ and

$$\sum_{\Gamma_C} f_\Gamma P_C = \sum_{\substack{\Gamma'_C \\ \text{or the trajectories present in the sample}}} f_{\Gamma'_C} .$$

It is in principle possible that when a very large number of cells are present, two different single cells could produce the same stochastic trajectory and for such cases, $\sum_{\Gamma_C} P_C \ln P_C$ will not vanish and $\sum_{\Gamma_C} f_\Gamma P_C$ will contain averages over multiple trajectories. However, occurrences of such events (e.g., the presence of pairs of identical stochastic trajectories) appear to be extremely rare for the rate constants and the ranges of the protein abundances we considered. We further tested this approximation by considering deterministic chemotactic signaling kinetics where the kinetics of signaling protein abundances only depend on the total protein abundances (as the kinetic rates are fixed for each cell), therefore, P_C=1 when the deterministic kinetic trajectory of abundances of signaling proteins is present and P_C=0, otherwise. When we used the same a priori uniform distribution for protein abundances as our stochastic simulations for the deterministic chemotactic kinetics, the qualitative results of the inferred $\hat{P}(\{n_q^{\text{total}}\})$ did not change compared to the stochastic simulations (Fig. S11). The small differences in the correlations shown in Fig. S11 between the stochastic and the deterministic simulations show the dominance of extrinsic noise fluctuations over intrinsic noise fluctuations in determining variations of protein abundances. These results also demonstrate that associating a unique stochastic trajectory to a single cell is a good approximation for the calculation of $\hat{P}(\{n_q^{\text{total}}\})$ in the stochastic simulations. We used the Levenberg-Marquardt algorithm in MATLAB to solve the nonlinear equations involving the Lagrange's multipliers.

Values of the constraints used when the chemotactic responses were constrained: We have considered average values, variances, and covariances of the variables characterizing the chemotactic response in E. coli. The variables are i) the adaptation time τ, ii) the precision of adaptation *s* and iii) the percentage variation of CheY-P about an optimal value *p*.

(i) Constraints for τ: The distribution of τ ($P(\tau)$) is measured in Ref. (25). We use the distribution for 100 μM of aspartate stimulation to calculate the average value and the variance of τ. $P(\tau)$ can be approximated fairly well with a normal distribution (χ^2 =

0.0024179), therefore, the higher moments beyond the second moment do not capture relevant information for τ. Therefore, we did not use any higher order moments to further constrain τ in the MaxEnt calculations.

(ii) Constraints for s: The cell population averaged value of s for wildtype RP437 strain was obtained from Alon et al (5). The experimental measurements for the variance or any higher order moments of *s* are not available from the literature. Therefore, we used an ad hoc small value (0.0005) for the variance of s. In order to study the sensitivity of the inferred $\hat{P}(\{n_q^{\text{total}}\})$ upon any change in the distribution of *s*, we investigated the change in $\hat{P}(\{n_q^{\text{total}}\})$ when a different value was used for the variance of *s* (Fig. S13).

(iii) Constraints for *p*: Study of the switching frequency of single E. coli cells for the transformed PS2001strains for different steady state concentrations of CheY-P was carried out by Cluzel et al (6). They found that a more than 30 % variation in CheY-P concentration about an optimal value leads to a dramatic decrease in the switching frequency. Since Ref. (6) used engineered cells, we do not have a direct access to the distribution of *p* for the wild type E. coli cells. We used a cell population averaged value of *p* at 20 with a standard deviation 5. We also varied the standard deviation to study the sensitivity of $\hat{P}(\{n_q^{\text{total}}\})$ on the shape of the distribution of p (Fig. S13).

(C) *Evaluation of* $\hat{P}(\{n_q^{\text{total}}\})$ *when total protein abundances are constrained*: We considered two cases: (a) cell population averaged total abundances of the chemotactic proteins were constrained. (b) The pair wise correlations between total abundances of chemotactic proteins were constrained along with the average values. We maximized the Shannon's Entropy,

$$S = -\sum_{\left\{n_q^{\text{total}}\right\}} P\left(\left\{n_q^{\text{total}}\right\}\right)\ln\left(P\left(\left\{n_q^{\text{total}}\right\}\right)\right) \tag{S9}$$

for both types of constraints.

Constraint on the mean: We constrained average values of the total protein abundances, i.e.,

$$\sum_{\left\{n_{\tilde{q}}^{\text{total}}\right\}} n_q^{\text{total}} P\left(\left\{n_{\tilde{q}}^{\text{total}}\right\}\right) = \overline{n_q}^{\text{expt}} \tag{S10}$$

,where, q = 1…6, represent the proteins Tar, CheA, CheY, CheR, CheB and CheZ, respectively. The distribution that maximizes Eq. (S9) in the presence of the constraints in Eq. (S10) is given by

$$\hat{P}\left(\left\{n_q^{\text{total}}\right\}\right) \propto \prod_q \exp\left(-n_q^{\text{total}} / \overline{n_q}^{\text{expt}}\right) \tag{S11}$$

We drew total protein abundances from an exponential distribution of the form in Eq. (S11) and then used stochastic signaling kinetics to generate the distributions of the variables characterizing chemotactic responses.

Constraint on the mean values, variances and covariances of total protein abundances:
Here the mean values (Eq. S10) as well as the pair-wise covaraiances ($C_{qq'}$) of the total protein abundances were constrained, i.e.,

$$\sum_{\left\{n_{\tilde{q}}^{\text{total}}\right\}} n_q^{\text{total}} n_{q'}^{\text{total}} P\left(\left\{n_{\tilde{q}}^{\text{total}}\right\}\right) - \overline{n_q}^{\text{expt}}\,\overline{n_{q'}}^{\text{expt}} = C_{qq'} \tag{S12}$$

The $\hat{P}(\{n_q^{\text{total}}\})$ that maximizes S in Eq. (S10) in the presence of constraints in Eqs. (S11-S12) is given by,

$$P\left(\left\{n_q^{\text{total}}\right\}\right) \propto \exp\left(\sum_{q,q'} n_q^{\text{total}} \cdot \mathbf{M} \cdot n_{q'}^{\text{total}}\right) + \sum_q \lambda_q n_q^{\text{total}} \tag{S13}$$

,where, $\mathbf{M}$ is a 6×6 symmetric matrix containing 21 independent Lagrange multipliers and $\{\lambda_q\}$ are 6 separate Lagrange multipliers arising from constraints for the mean values. For BL model, $\mathbf{M}$ is a 5×5 matrix with 15 independent elements and there are 5 different λ_qs.

We have represented the distribution in Eq. (S13) as a multivariate Gaussian distribution of the form

$$P\left(\left\{n_q^{\text{total}}\right\}\right) \propto \exp\left(-\frac{1}{2}\sum_{q,q'}\left(n_q^{total} - \overline{n_q}^{\text{expt}}\right)\cdot \mathbf{C}^{-1} \cdot \left(n_{q'}^{total} - \overline{n_{q'}}^{\text{expt}}\right)\right) \tag{S14}$$

where, $\mathbf{C}$ is the 6×6 covariance matrix in Eq (S12). Thus, the Lagrange multipliers in $\mathbf{M}$ and $\{\lambda_q\}$ are determined from the mean values and the $\mathbf{C}$ matrix obtained from the experiments or constraints.

Kollmann et al (1) measured covariances between CheZ, CheY and CheA, CheY pairs. Ref. (1) proposed a log-normal distribution for the describing the joint distribution for all

the total protein abundances. The proposed log-normal distribution agrees well with the measured distributions in Kollmann et al., and, we found that when we used that distribution it reproduced the chemotactic responses reasonably well (Fig. S7 red plots). So, we used the values computed from the log-nornal distribution to constrain the covariances in our calculation.

According to Ref. (1)

$$n_q^{\text{total}} \approx \overline{n}_q^{\text{expt}} \left(\lambda r + 0.2\sqrt{\lambda} \cdot \xi_q \right), \qquad \text{(S15)}$$

where λ is the protein overexpression factor (should not be confused with λ_q), for the wild type RP437 strain λ=1. ξ_q is a Gaussian variable with zero mean and unit variance and r is a Log normal variable with unit mean. Using Eq. (S15) we calculated the **C** matrix as

$$C_{qq'} \approx 0.25 \times \overline{n}_q^{\text{expt}} \overline{n}_{q'}^{\text{expt}} + \rho \delta'_{qq} \qquad \text{(S16)}$$

, where, ρ=0.04. We used the C matrix in Eq. (S16) to calculate the distribution in Eq. (S14). We simulated the distribution in Eq. (S16) by drawing random numbers from the multivariate Gaussian distribution given by Eq. (S14).

IV. Evaluation of the minimal number of constraints required to reproduce the observed chemotactic response in E. coli

We drew intuition for constructing the case that will require the minimum number of constraints by considering the form of the C matrix in Eq. (S16). The C matrix in Eq. (S16) produces a strong Pearson correlation co-efficient of about 0.85 for any two pairs. When we approximate Eq. (S16) by,

$$C_{qq'} \approx 0.25 \times \overline{n}_q^{\text{expt}} \overline{n}_{q'}^{\text{expt}} \qquad \text{(S17)}$$

then Pearson correlation co-efficient between protein pairs is exactly 1. The C matrix in Eq. (S17) is singular with one non-zero eigenvalue equal to $e_1 = 0.25 \times \sum_{q=1}^{6} (\overline{n}_q^{\text{expt}})^2$, and the rest of the eigenvalues are zero, i.e., $e_2 = \cdots = e_6 = 0$. Using the eigenvectors of the **C** matrix in Eq. (S17) it can be shown that when any total protein abundance, (say n_1^{total}), follows a Gaussian distribution with a mean $\overline{n}_1^{\text{expt}}$ and a variance, $C_{11} = 0.25 \times (\overline{n}_1^{\text{expt}})^2$, and rest of the total protein abundances are related as follows:

$$\bar{n}_{q-1}^{\text{expt}}(n_q^{\text{total}} - \bar{n}_q^{\text{expt}}) = \bar{n}_q^{\text{expt}}(n_{q-1}^{\text{total}} - \bar{n}_{q-1}^{\text{expt}}) \quad \text{(S18)}$$

, where, q=2..6, then the resulting distribution produces the C matrix in Eq. (S17). The relation in Eq. (S18) indicates a strong dependence between the proteins, e.g., protein 2 is regulated by protein 1, then protein 3 is regulated by protein 2, and so on. Thus, it indicated as long as, the proteins are connected to each other following a linear chain describing Eq. (S18), one could reproduce the correlation in Eq. (S17). The ordering of the proteins is not important as long as they are connected to the nearest neighbors. Next we checked how well the distribution of total protein abundances constructed using Eq. (S17) and mean values from Eq. (S10) can reproduce the chemotactic responses. We found the distribution reproduces the observed response reasonably well (Figs. S9-S10 maroon plots). Therefore, it indicates that the minimum number of constraints in this case would be composed of the mean values of the total protein abundances (6 in total) and the variance for one protein (say C_{11}).

Now we consider the C matrix in Eq. (S16), which is not a singular matrix, therefore, the strict equality between the protein abundances as given by Eq. (S18) is relaxed. However, drawing from the intuition developed from the above calculations, we constrain a set of pair correlations that will connect the proteins in a linear chain, e.g., the covariances between, Tar-CheA, CheA-CheY, CheY-CheR, CheR-CheB, and CheB-CheZ. We also constrained the mean values of the proteins as well. We then evaluated the corresponding multivariate Gaussian distribution for $\hat{P}(\{n_q^{\text{total}}\})$ that generates the constrained covariances and average values, and then use the distribution to generate the chemotactic responses (Fig. S7 and Fig S9 blue plots, Fig. S10 both blue and brown plots). We have studied two values of ρ in Eq. (S16), 0.01 and 0.04, respectively. For $\rho = 0.01$, the nearest neighbor correlation coefficients are 0.95 while for $\rho = 0.04$, the nearest neighbor correlation coefficients are 0.83. We found that for $\rho = 0.01$, the distributions of τ, s, and, p are in reasonable agreement with the experiments (Figs. S9-S10). For $\rho = 0.04$, the distribution for p becomes slightly broader. Thus, as long as we impose a strong correlation between the protein abundances by linking protein abundances in a linear chain, the resulting $\hat{P}(\{n_q^{\text{total}}\})$ reproduces the chemotactic responses reasonably well. Next we further tested the sensitivity of the linked network by removing a link, e.g., we constrained the covariances between, Tar-CheA, CheA-CheY, CheY-CheR, and CheR-CheB were constrained but the covariance between CheB-CheZ *was not constrained*.

Results for the one deleted link case: In this case, instead of 17 (6 mean values, 6 variances, and 5 covariances) constraints as in the linked case we will have 16 constraints (6 mean values, 6 variances, and 4 covariances). Both for $\rho = 0.01$ or $\rho = 0.04$, deletion of a link produces a large change in the distribution of p, making it broader (Figs. S7 and S9 indigo plots) suggesting a larger fraction of the E. coli cell will possess non-functional flagellar motors. Thus, this test further supports the mechanism, that as long as the total

protein abundances are strongly linked by pair-correlations through the constraints, the resulting population will capture the observed chemotactic response reasonably well.

V. Calculation of the χ^2 distance to quantify comparison between the chemotactic responses obtained from inferred MaxEnt distributions and the experiments

The experimental values are shown in red in Table S5A. The values that we estimated are shown in green in that table. The standard errors (σ) for the assumed mean values are assumed to be of the same order as the mean values. We calculated the chi-square (χ^2) given by,

$$\chi^2 = \sum_{i=1}^{5} \left(\frac{\overline{O^i_{\text{inferred}}} - \overline{O^i_{\text{expt}}}}{\sigma_{\overline{O^i_{\text{expt}}}}} \right)^2 \qquad \text{(S19)}$$

where the overbar indicates average values, and σ indicates the variance. The O^i is the i^{th} variable describing the chemotactic responses and $\sigma_{\overline{O^i_{\text{expt}}}}$ is the standard error in the variable. The subscripts "inferred" and "expt" denote the values obtained using the inferred distribution and the experimental measurements, respectively. Smaller values of χ^2 indicate a better agreement. The χ^2 values of the inferred distributions are shown in Table S5B-S5D.

Table S1A: Average values of protein abundances used in the model

Species	Concentration (μM)
Receptor Total (T=Tar + Tsr)	17.8
CheA	5.3
CheB	0.28
CheR	0.16
CheY	9.7
CheZ (MBL and FT)	3.8

Cell volume is 1.4 fl. The average concentrations of the chemotactic proteins for the RP437 strain have been taken from (9).

For a reaction line $\text{Tar}_m^{\text{inact}} \underset{k_{-1}}{\overset{k_1}{\rightleftarrows}} \text{Tar}_m^A$, we have defined $a_m = k_1/(k_1 + k_{-1})$ such that in the steady state $\text{Tar}_m^A = a_m \cdot \text{Tar}_m^{\text{Total}}$. In the absence of the ligands we have assumed that

$a_m = m / m_{\text{Max}}$. In the presence of 100 μM aspartate, we assume that all the Tar molecules are ligand bound. The values of a_m used are shown below. We chose these values in order to match the average adaptation time in our model to the one quoted in the experiment (25).

Table S1B: The activation probabilities

Reactions	a(L = 0 μM)	a(L =100 μM)
$T_1^{inact} \rightarrow T_1^A$	0.125	0.0014
$T_2^{inact} \rightarrow T_2^A$	0.5	0.0115
$T_3^{inact} \rightarrow T_3^A$	0.874	0.056
$T_4^{inact} \rightarrow T_4^A$	1.0	1.0

Table S2A: Reactions for MBL model

Reactions	Michaelis-Menten Constant	Rates
$T_m + \text{CheR} \underset{k_{-1}}{\overset{k_1}{\rightleftarrows}} T_m\text{-CheR} \xrightarrow{k_r} T_{m+1} + \text{CheR}$	$K_r=(k_{-1} + k_r)/k_1$ = 0.099 μM	$k_r = 0.39\ s^{-1}$
$T_m^A + \text{CheB-P} \underset{k_{-1}}{\overset{k_1}{\rightleftarrows}} T_m^A\text{-CheB-P} \xrightarrow{k_b} T_{m-1}^A + \text{CheB-P}$	$K_b=(k_{-1} + k_b)/k_1$ = 2.5 μM	$k_b = 6.3\ s^{-1}$
$\text{CheA} + T^A \rightarrow \text{CheA-P} + T^A$		$k_p = 50\ \mu M^{-1}s^{-1}$
$\text{CheB} + \text{CheA-P} \rightarrow \text{CheB-P} + \text{CheA}$		$a_b = 3\ \mu M^{-1}s^{-1}$
$\text{CheB-P} \rightarrow \text{CheB}$		$d_b = 1.0\ s^{-1}$
$\text{CheY} + \text{CheA-P} \rightarrow \text{CheY-P} + \text{CheA}$		$a_y = 100\ \mu M^{-1}s^{-1}$
$\text{CheY-P} \rightarrow \text{CheY}$		$d_y = 0.1\ s^{-1}$
$\text{CheY-P} + \text{CheZ} \rightarrow \text{CheY} + \text{CheZ}$		$k_Z = 7.8\ \mu M^{-1}s^{-1}$

The rate constants are taken from Kollmann et al.

Table S2B: Reactions for FT model

Reactions	Michaelis-Menten Constant	Rates
$T_m + \text{CheR} \underset{k_{-1}}{\overset{k_1}{\rightleftarrows}} T_m\text{-CheR} \xrightarrow{k_r} T_{m+1} + \text{CheR}$	$K_r=(k_{-1} + k_r)/k_1$ = 0.099 μM	$k_r = 0.39\ s^{-1}$
$T_m + \text{CheB-P} \underset{k_{-1}}{\overset{k_1}{\rightleftarrows}} T_m\text{-CheB-P} \xrightarrow{k_b} T_{m-1} + \text{CheB-P}$	$K_b=(k_{-1} + k_b)/k_1$ = 2.5 μM	$k_b = 6.3\ s^{-1}$
$\text{CheA} + T^A \rightarrow \text{CheA-P} + T^A$		$k_p = 50\ \mu M^{-1}s^{-1}$
$\text{CheB} + \text{CheA-P} \rightarrow \text{CheB-P} + \text{CheA}$		$a_b = 3\ \mu M^{-1}s^{-1}$

CheB-P $\rightarrow$ CheB		$d_b = 1.0\ s^{-1}$
CheY + CheA-P $\rightarrow$ CheY-P + CheA		$a_y = 100\ \mu M^{-1}s^{-1}$
CheY-P $\rightarrow$ CheY		$d_y = 0.1\ s^{-1}$
CheY-P + CheZ $\rightarrow$ CheY + CheZ		$k_Z = 7.8\ \mu M^{-1}s^{-1}$

Table S2C: Reactions for BL model

Reactions	Michaelis-Menten Constant	Rates
$T_m + \text{CheR} \underset{k_{-1}}{\overset{k_1}{\rightleftharpoons}} T_m\text{-CheR} \xrightarrow{k_r} T_{m+1} + \text{CheR}$	$K_r=(k_{-1} + k_r)/k_1 = 0.099\ \mu M$	$k_r = 0.39\ s^{-1}$
$T_m^A + \text{CheB-P} \underset{k_{-1}}{\overset{k_1}{\rightleftharpoons}} T_m^A\text{-CheB-P} \xrightarrow{k_b} T_{m-1}^A + \text{CheB-P}$	$K_b=(k_{-1} + k_b)/k_1 = 2.5\ \mu M$	$k_b = 6.3\ s^{-1}$ †
CheA + $T^A \rightarrow$ CheA-P + T^A		$k_p = 50\ \mu M^{-1}s^{-1}$
CheB + CheA-P $\rightarrow$ CheB-P + CheA		$a_b = 3\ \mu M^{-1}s^{-1}$
CheB-P $\rightarrow$ CheB		$d_b = 1.0\ s^{-1}$
CheY + CheA-P $\rightarrow$ CheY-P + CheA		$a_y = 100\ \mu M^{-1}s^{-1}$
CheY-P $\rightarrow$ CheY		$d_y = 30\ s^{-1}$

† The K_b and k_b values used by Kollmann et al for the BL model are 16 μM and 16 s^{-1} respectively. We have used the same rate constants for all the three models to facilitate comparison across them.

Table S3: Comparison of the average values of protein abundances generated by the MaxEnt distribution when different combinations of the chemotactic outputs (τ, τ^2, s, s^2, p, p^2) are constrained to the cell population averages measured in experiments.

A: Experiments (9)

	Tar+Tsr molecules/ cell	CheA molecules/ cell	CheY molecules/ cell	CheR molecules/ cell	CheB molecules/ cell	CheZ molecules/ cell
	15000 ± 1700	4452 ± 920	8148 ± 310	140 ± 10	240 ± 10	3200 ± 90

B: The values quoted are for MBL model.

Constraints	**Tar+Tsr molecules / cell**	**CheA molecules / cell**	**CheY molecules / cell**	**CheR molecules / cell**	**CheB molecules / cell**	**CheZ molecules / cell**
$\overline{\tau} = 245$ s	46698	14584	24404	786	466	10198
$\overline{p} = 20$	46318	13025	21015	667	547	12543
$\overline{s} = 0.02$	48933	15409	23570	838	465	9566
$\overline{\tau} = 245$ s $\overline{s} = 0.02$ $\overline{p} = 20$ $\overline{\tau^2} = 62323$ s^2 $\overline{p^2} = 425$	59991	12693	24670	504	538	12909
$\overline{s} = 0.02$ $\overline{p} = 20$ $\overline{\tau^2} = 62323$ s^2 $\overline{p^2} = 425$ $\overline{s^2} = 0.0005$	60033	13023	24630	491	545	13051

Table S4: Pearson correlations between protein abundances.
Average values of s, p, τ, τ^2, and p^2 were constrained in the MaxEnt calculation.

Protein pair	Sign of Pearson correlation from the MaxEnt calculation		Single Cell Experiment (Fig. 2, Kollmann et al., Nature, 2005)	In vitro assay of cloned gene pairs (Fig. 1, Lovdok et al. , PloS Biol., 2009) (26)	Bioinformatic Analysis of pairwise gene co-occurrence (Table 1, Lovdok et al. , PloS Biol., 2009) (26)
	MBL	FT			
Tar-CheA (^)	-	-			+ (10.5)
Tar-CheY	-	+			+ (1.9*)
Tar-CheR	+	-			+ (16.8)
Tar-CheB	+	+			+(2.3*)

Tar-CheZ	+	+			+(<1*)
CheA-CheY (^)	-	-	+		+(15.7)
CheA-CheR (^)	-	+			+(3.9*)
CheA-CheB (^)	+	-			+(15.1)
CheA-CheZ (^)	+	-			+(32.5)
CheY-CheR	+	-			+(1.9*)
CheY-CheB	+	+		+	+(15.0)
CheY-CheZ	+	+	+	+	+(90.0)
CheR-CheB	-	-		+	+(28.6)
CheR-CheZ	+	-			0
CheB-CheZ	-	+			+(<1*)

* Indicates small pair-wise occurrence in bacterial genomes.
^ Indicates protein pairs encoded by genes in the same operon (*meche*).
Signs marked in blue and red indicate agreement and disagreement, respectively, between MaxEnt predictions and experiments.
Rows shaded with blue denote positive correlations between protein abundances predicted by the MaxEnt approach for the MBL model.

Table S5: Table for the χ^2 for the average chemotactic outputs obtained from the distributions of the τ, p, and s in Fig S7-S8 and the experimentally observed values.

A: Values obtained from the Experimental measurements

	$\bar{\tau}$ sec	$\overline{\tau^2}$ sec^2	$\sigma_{\bar{\tau}}$ sec	$\sigma_{\overline{\tau^2}}$ sec^2	$\bar{s}$	$\bar{p}$	$\overline{p^2}$	$\sigma_{\bar{s}}$	$\sigma_{\bar{p}}$	$\sigma_{\overline{p^2}}$
Experiments	250.4	65092	18.6	9205	0.02	20	425	0.01	10	250

B: Multivariate Gaussian (constrained means, variances and correlations, Fig 4 main text and Fig S8)

	$\bar{\tau}$ sec	$\overline{\tau^2}$ sec^2	$\bar{s}$	$\bar{p}$	$\overline{p^2}$	χ^2
MBL (Total 27 constraints)	277	94338	0.03	24	1026	20.0
BL (Total 21 constraints)	226	59272	0.05	49	4045	229
FT (Total	226	65487	0.3	31	1500	829

27 constraints)						

C: χ^2 for the average chemotactic outputs obtained from the distributions of the phenotypes in Fig S7 from the experiments.

MaxEnt distributions for MBL model	$\bar{\tau}$ sec	$\overline{\tau^2}$ sec^2	$\bar{s}$	$\bar{p}$	$\overline{p^2}$	χ^2
Exponential (6 constraints)	401	366248	0.09	111	35228	20641
Gaussian (27 constraints)	277	94338	0.03	24	1026	20.0
Nearest Neigbor (17 constraints, $\rho = 0.04$)	280	105020	0.04	44	3821	215
Nearest Neigbor (17 constraints, $\rho = 0.01$)	270	82978	0.03	24	1048	13
One Deleted link (16 constraints, $\rho = 0.04$)	284	113332	0.04	65	9477	1366
One Deleted link (16 constraints, $\rho = 0.01$)	278	99564	0.04	61	8125	984

D: χ^2 for the average chemotactic outputs obtained from the distributions of the phenotypes when the protein numbers are drawn from log-normal distribution (Kollmann et al (1)).

MaxEnt distributions for MBL model	$\overline{\tau}$ sec	$\overline{\tau^2}$ sec^2	$\overline{s}$	$\overline{p}$	$\overline{p^2}$	χ^2
Log-normal distribution	264	80620	0.06	26	1158	30

Table S6: **The χ^2 of the first and second order cumulants of CheY, CheZ and CheA obtained from the MaxEnt distribution of the MBL model when τ, τ^2, s, p, p^2 are constrained to the experimental value.**

	Average$_{MBL}$ $\overline{O^i_{dist}}$	**Average$_{expt}$** $\overline{O^i_{\text{expt}}}$	**Error$_{expt}$** $\sigma_{\overline{O^i_{\text{expt}}}}$	$\chi^2 = \sum_{i=1}^{8}\left(\frac{\overline{O^i_{\text{inferred}}} - \overline{O^i_{\text{expt}}}}{\sigma_{\overline{O^i_{\text{expt}}}}}\right)^2$
$\overline{\text{CheY}}$	24670	8148	507	
$\overline{\text{CheZ}}$	12909	3192	223	
$\overline{\text{CheA}}$	12693	4452	233	32500
$\overline{\text{CheY}^2}$	7.80057e+08	7.79465e+07	9.1372e+06	
$\overline{\text{CheZ}^2}$	1.89109e+08	1.2914e+07	2.0356e+06	
$\overline{\text{CheA}^2}$	2.25765e+08	2.22611e+07	2.42987e+06	
$\overline{\text{CheY}\bullet\text{CheZ}}$	3.40111e+08	3.19421e+07	5.3621e+06	
$\overline{\text{CheY}\bullet\text{CheA}}$	3.00493e+08	3.92766e+07	3.86588e+06	

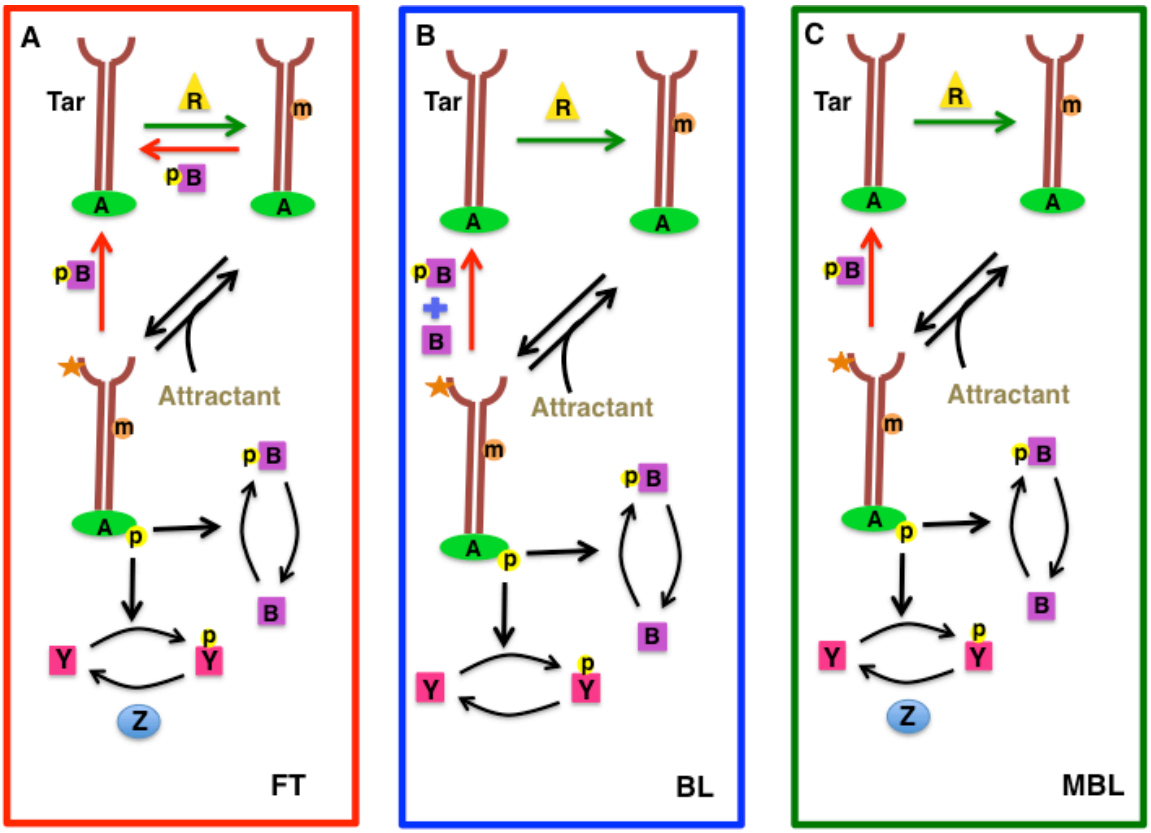

Fig. S1 Three models for *E. coli* chemotaxis. (A) The Fine tuned model (FT), originally proposed by Knox et al and Hauri and Ross, shows robust adaptation only for a small region in the parameter space. In this model the aspartate receptors (Tar) can shuttle between an active (denoted by the orange star) and an inactive conformation. The probability of the receptors to be in an active conformation depends on their state of methylation. Pair of enzymes namely CheR (R) and CheB-P (B) add and remove methyl groups from the receptors. CheB-P can demethylate receptors regardless of *their state of activity*. The Tar receptors form complexes with a kinase CheA (A). CheA can phosphorylate itself with a rate proportional to the abundance of the active Tar. Phosphorylated CheA can transfer its phosphoryl group (PO_4) either to the kinase CheB, rendering it capable of demethylation, or to another response regulatory protein called CheY (Y). Upon receiving the phosphoryl group from CheA, CheY renders itself active. Active form of CheY (CheY-P) diffuses across the cell and binds to the flagella motors causing them to tumble. The phosphatase CheZ (Z) de-activates the active form CheY. **(B)** Barkai Leibler model (BL) was put forward to explain robust adaptation in the chemotactic network of bacterial *E. coli*. Unlike FT model, CheB, both the unphosphorylated and the phosphorylated form, demethylates only the *active* Tar receptors. This model also lacks the phosphatase CheZ. **(C)** MBL model proposed by Kollmann et al., albeit for two differences, is exactly similar to the BL model. The differences are i) Unlike $CheB^T$ (CheB-P and CheB), only the *phosphorylated* form of

CheB can de-methylate the active receptors in this model. ii) The dephosphorylation of the active CheY is done by the phosphatase called CheZ (Z). The presence of this phosphatase makes the steady state of CheY-P relatively robust to the concerted over expression of the chemotactic proteins. We use the figure (Fig. 1) from Mukherjee et al, (8) here for the convenience of the readers.

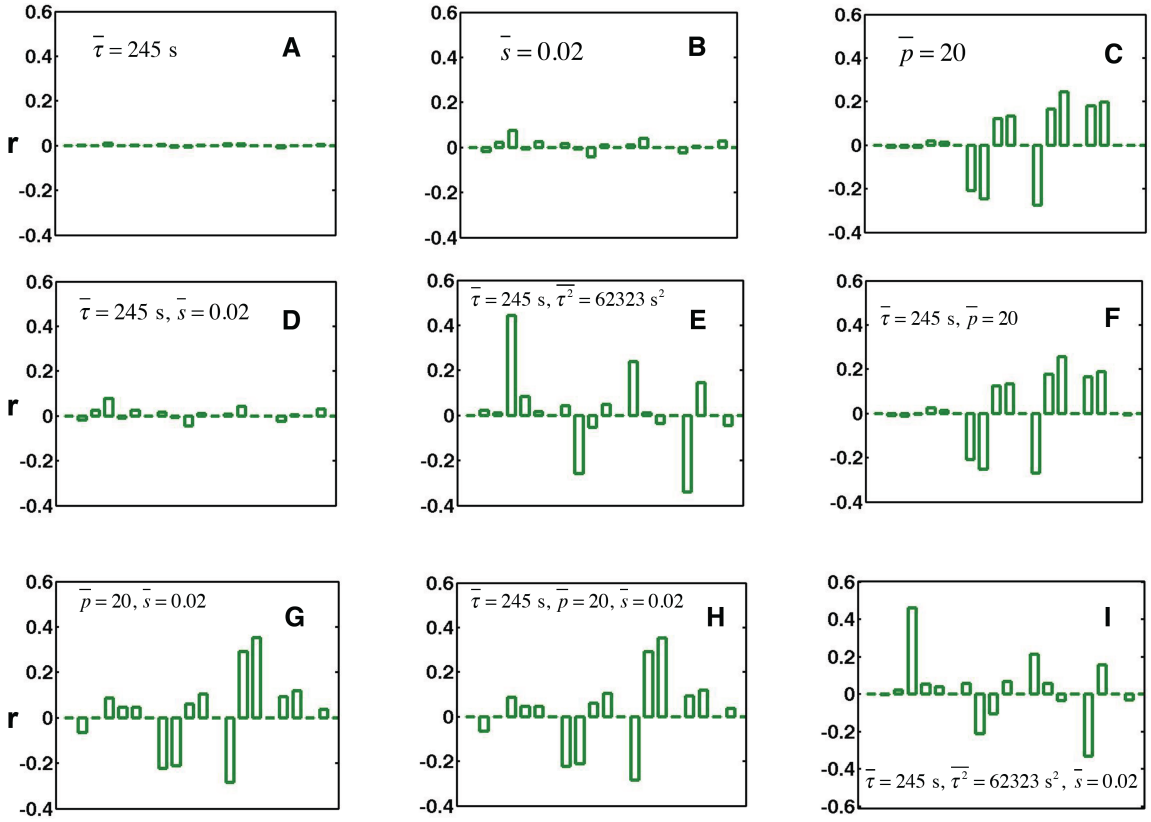

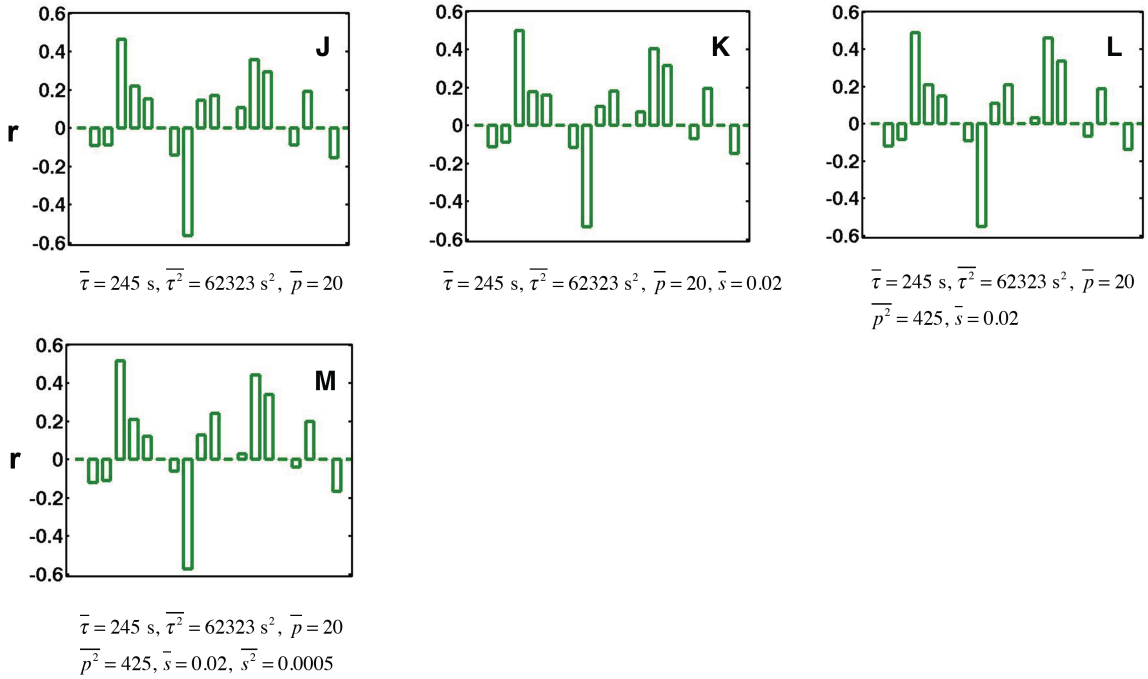

Fig S2: Pearson correlations are shown for the MBL for different combinations of the chemotactic constraints. The green bars from left to right represent the correlation co-effiecients between Tar-Tar, Tar-CheA, Tar-CheY, Tar-CheR, Tar-CheB, Tar-CheZ, CheA-CheA, CheA-CheY, CheA-CheR, CheA-CheB, CheA-CheZ, CheY-CheY, CheY-CheR, CheY-CheB, CheY-CheZ, CheR-CheR, CheR-CheB, CheR-CheZ, CheB-CheB, CheB-CheZ and CheZ-CheZ respectively **(A)** The average value of the adaptation time is constrained to the experimental average of 245 s. **(B)** The average value of the precision of adaptation is constrained to the experimental value of 0.02. **(C)** The average value of the percentage variation in the steady states of CheY-P is constrained to 20%. **(D)** The average value of the adaptation time and the precision of adaptation are both constrained to the experimental values of 245 s and 0.02. **(E)** The average and the second moment of the adaptation time are constrained to 245s and 62323s^2 respectively. **(F)** The average value of the adaptation time and the percentage variation in the steady state of CheY-P are constrained to 245s and 20 %. **(G)** The steady state variation of the CheY-P protein and the precision of adaptation are constrained to 20% and 0.02 respectively. **(H)** All the three chemotactic outputs, the adaptation time, precision of adaptation and the variation in the steady state of CheY-P from the optimal value are constrained to 245s, 0.02 and 20% respectively. **(I)** The average adaptation time, the second moment of the adaptation time and the precision of adaptation are constrained to 245 s, 62323 s^2 and 0.02 respectively. **(J)** The average value of the adaptation time, the second moment of the adaptation time and the percentage variation of the steady state of CheY-P are constrained to 245 s, 62323 s^2 and 20% respectively. **(K)** The average value of the adaptation time, its second moment, the precision of adaptation and the variation in the

steady state of CheY-P are constrained to 245 s, 62323 s^2 , 0.02 and 20%. **(L)** The adaptation time, the second moment of the adaptation time, the precision of adaptation, the variation in the steady state of CheY-P and its second moment are all constrained to 24s s, 62323 s^2, 0.02, 20% and 425 respectively. **(M)** On top of the 5 constraints in S5 (L) we added an extra constraint of 0.0005 on the second moment of the precision of adaptation. We show the difference, $r = r_{MaxEnt} - r_{uni}$ for different protein pairs, where, r_{uni} and r_{MaxEnt} refer to the Pearson correlation calculated for the *a priori* uniform and the MaxEnt distribution, respectively. The number of samples for all the cases is 70,000.

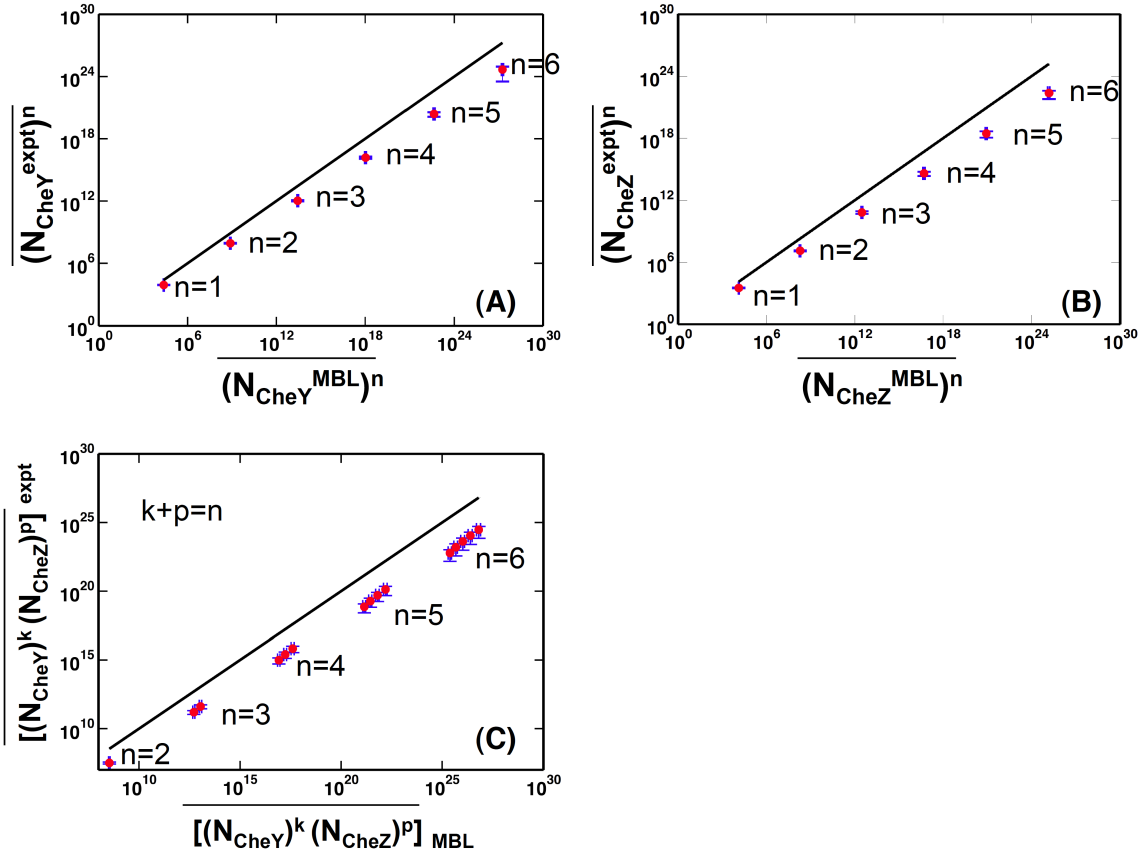

Fig S3: A comparison of individual and cross moments of CheY and CheZ when six chemotactic outputs are constrained in the MBL model. We calculate all the moments up to the sixth order. The constraints imposed for all the plots above are $\overline{\tau} = 245$ s, $\overline{\tau^2} = 62323$ s^2, $\overline{s} = 0.02$, $\overline{p} = 20$, $\overline{p^2} = 425$, $\overline{s^2} = 0.0005$.

(A) Comparison of the moments of CheY abundances calculated from the MaxEnt distribution with the data from single cell experiments in Ref.(1). The y=x line (solid black) is shown for comparison. **(B)** Similar comparison as in (A) for CheZ abundances. **(C)** Similar comparison as in (A) for the joint distribution of CheZ and CheY abundances. The y=x line (solid black) is shown for comparison.

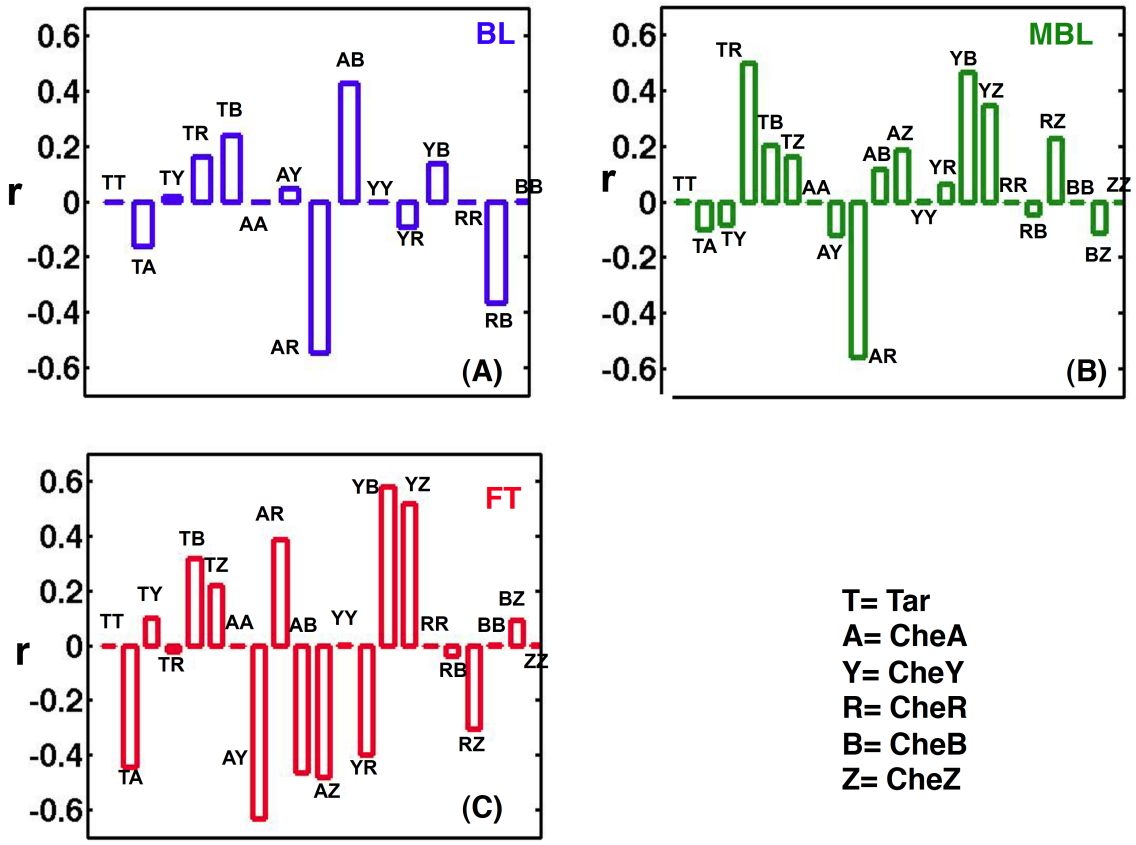

Fig. S4: Pearson correlations between protein abundances for the BL, MBL and FT models. We constrained mean values of τ, τ^2, s, p, and, p^2 to the respective values measured in experiments, i.e., $\overline{\tau} = 245$ s, $\overline{\tau^2} = 62323.5$ s^2, $\overline{s} = 0.02$, $\overline{p} = 20\%$, and p^2= 425. We show the difference, $r = r_{MaxEnt} - r_{uni}$ for different protein pairs, where, r_{uni} and r_{MaxEnt} refer to the Pearson correlation calculated for the *a priori* uniform and the MaxEnt distribution, respectively for **(A)** BL **(B)** MBL **(C)** FT models. The number of samples in all the cases is 70,000.

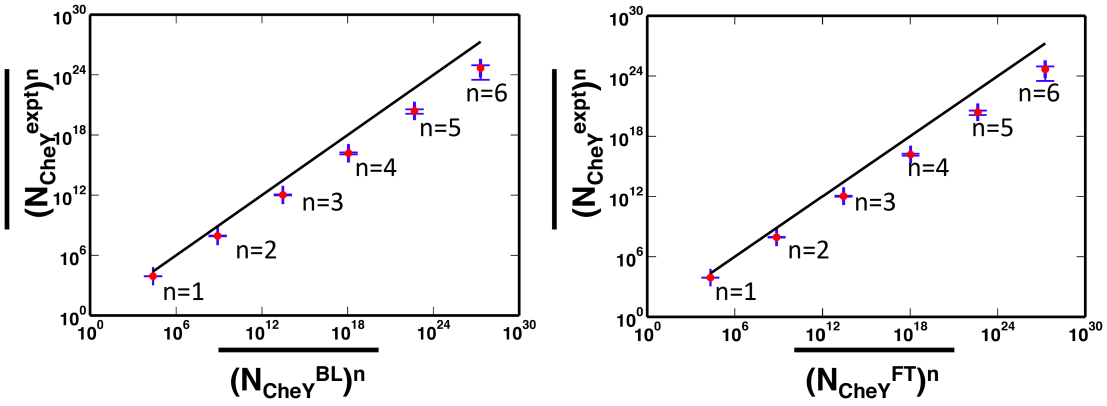

Fig S5: Comparison between moments of MaxEnt distribution and single cell experiments for the BL (left) and the FT (right) model. We constrained mean values of τ, τ^2, s, p, and, p^2 to the respective values measured in experiments, i.e., $\overline{\tau} = 245$ s, $\overline{\tau^2} = 62323.5$ s^2, $\overline{s} = 0.02$, $\overline{p} = 20\%$, and $p^2 = 425$. The MaxEnt distributions for abundance of CheY for both the models BL and FT, are broader than the experiments. The y=x line (solid black) is shown as a reference. The number of samples used is 70,000.

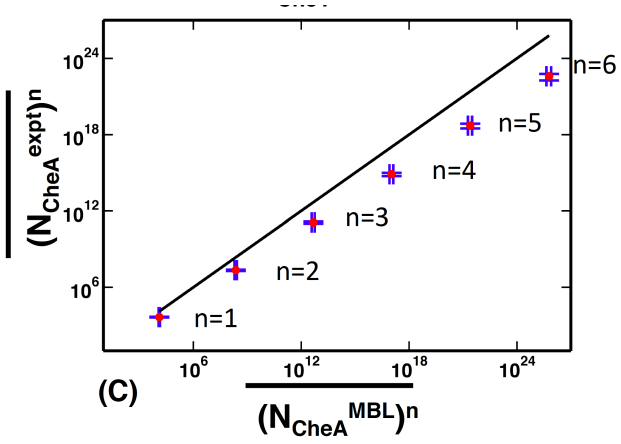

Fig S6: Comparison between moments of MaxEnt distribution for CheA abundance and single cell experiments for the MBL. We constrained mean values of τ, τ^2, s, p, and, p^2 to the respective values measured in experiments, i.e., $\overline{\tau} = 245$ s, $\overline{\tau^2} = 62323.5$ s^2, $\overline{s} = 0.02$, $\overline{p} = 20\%$, and $p^2 = 425$. The MaxEnt for abundances of CheA for the MBL model is broader than the experiments. The y=x line (solid black) is shown as a reference. The number of samples used is 70,000.

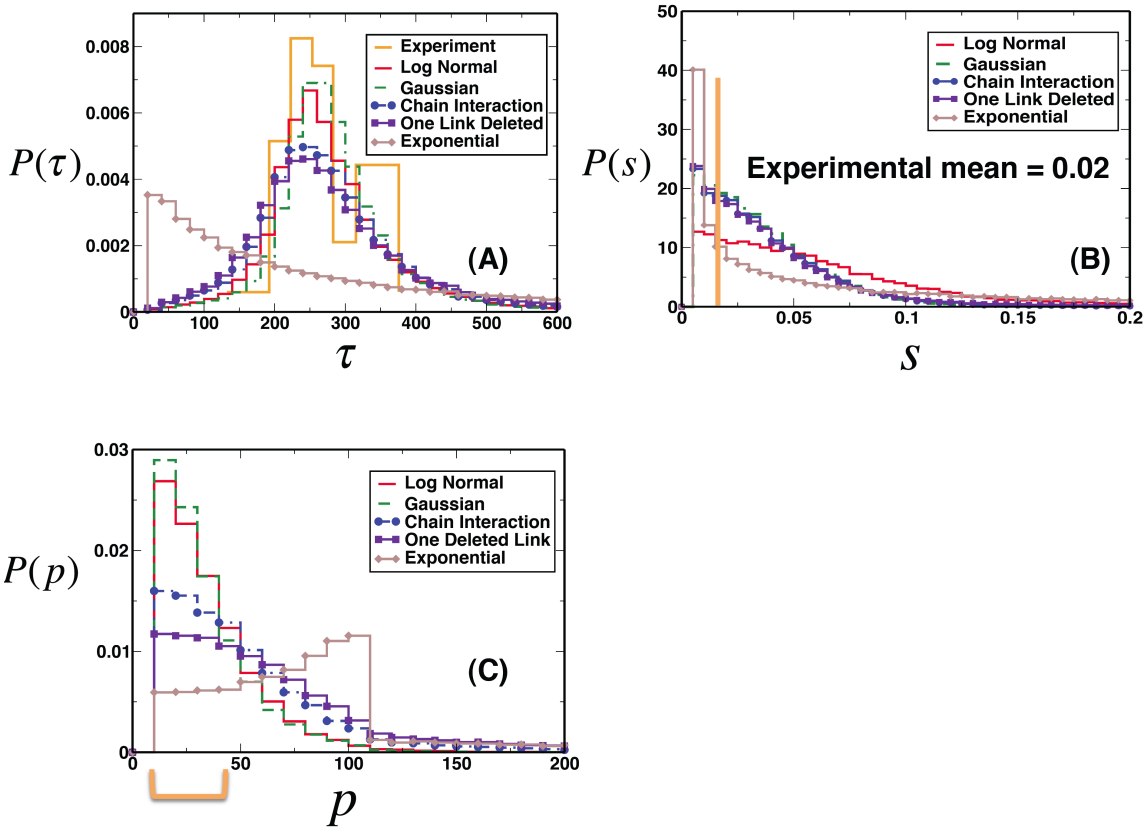

Fig S7: Distributions of τ, p, and s, when the total protein abundances are drawn from different MaxEnt distributions obtained by imposing different types of constraints on the total protein abundances. (A) Shows the distribution of the adaptation time when $\{n_q^{total}\}$ are drawn from the Log-normal distribution (**Log Normal**: solid red) as proposed by Kollmann et al. (1); multivariate Gaussian distribution (**Gaussian**: dashed green) where all the pair covariances as well as the mean values are constrained; the Gaussian distribution generated by constraining the covariances between the pairs: (Tar-CheA, CheA-CheY, CheY-CheR, CheR-CheB, and CheB-CheZ), as well as the variances and the mean values of the protein abundances (**Chain Interaction**: dashed blue with solid blue circles); the distribution with the constraints used in the previous case except the pair CheB-CheZ was not constrained (**One Deleted Link**: solid indigo with solid indigo squares); and exponential distribution which was generated when only the mean total abundances were constrained (**Exponential**: solid brown with brown diamonds). The orange graph is the experimental distribution of the adaptation time obtained from Min et al. (25). **(B)** Shows the distribution of the precision of adaptation when the protein numbers for the same types of distributions considered in (A) which are shown with the same color scheme. The orange vertical bar indicates the experimentally measured average precision of adaptation. **(C)** Shows the distribution of the variation of the steady state of the CheY-P protein from an optimal value or *p* for the same types of distributions considered in (A) which are shown with the same color scheme. The orange

square bracket indicates the operational range of the flagella motors. The number of samples used is 37,000 for all the results shown above.

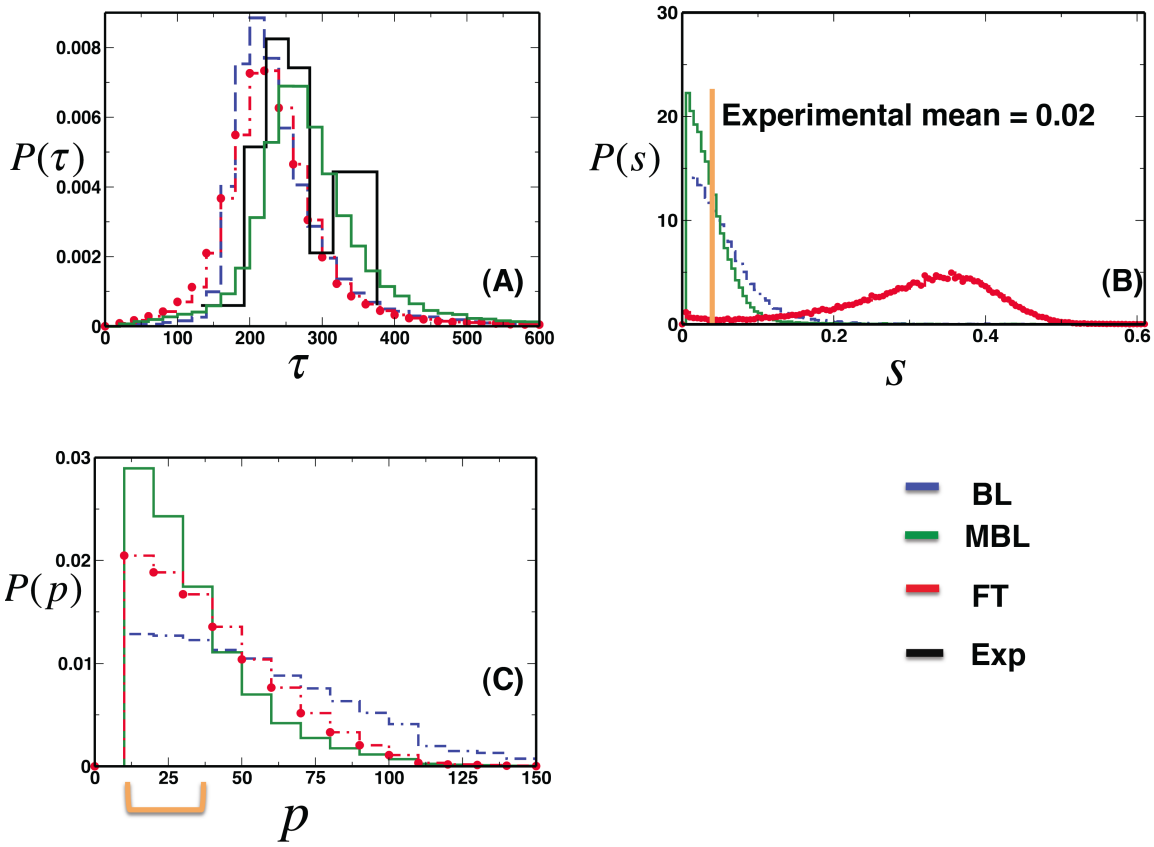

Fig S8: Shows the distributions of τ, p, and s for BL, MBL and FT models when the mean and the pair correlations of the chemotactic proteins are constrained to the experimental value: (A) Distribution of the adaptation time for BL (dashed blue), MBL (solid green) and FT model (dashed red with solid red circles) when the mean and the pair correlations between the chemotactic proteins are constrained. The plot in solid black is the experimentally observed adaptation time (25). **(B)** Distribution of the precision of adaptation for BL (dashed blue), MBL (solid green) and FT model (dashed red with solid red circles) when the mean and the pair correlations between the chemotactic proteins are constrained. The vertical line in orange indicates the experimental average precision. **(C)** Distribution of the percentage variation of the steady state of CheY-P from an optimal value for BL (dashed blue), MBL (solid green) and FT model (dashed red with solid red circles) when the mean and the pair correlations between the chemotactic proteins are constrained. The square bracket in orange shows the working range of the flagella motors. The number of samples used is 37,000.

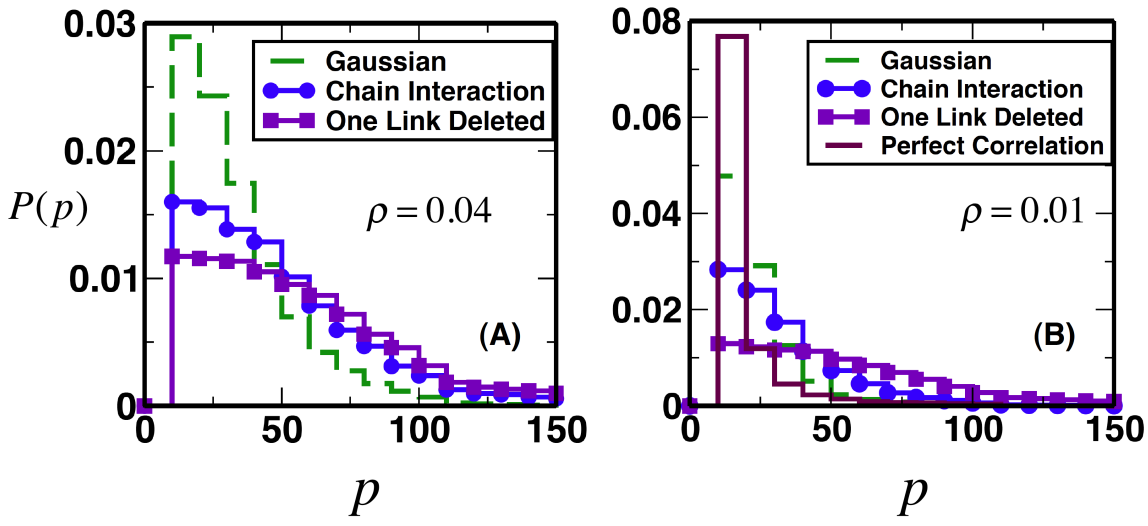

Fig S9: A comparison of the distribution of *p* for different MaxEnt distributions for two different strength of ρ in Eq. (S16). (A) Shows the distribution of *p* when the total protein abundances are drawn from a multivariate Gaussian distribution (**Gaussian**: dashed green) where all the pair covariances as well as the mean values are constrained; the Gaussian distribution generated by constraining the covariances between the pairs: (Tar-CheA, CheA-CheY, CheY-CheR, CheR-CheB, and CheB-CheZ), as well as the variances and the mean values of the protein abundances (**Chain Interaction**: dashed blue with solid blue circles); the distribution with the constraints used in the previous case except the pair CheB-CheZ was not constrained (**One Deleted Link**: solid indigo with solid indigo squares) when ρ=0.04 is used in the correlation matrix **C**. **(B)** Shows the same plot as in (A) for ρ=0.01. We also show the case (solid Maroon) when the constrained covariances and variances were taken from the C matrix in Eq. (S17) where ρ=0 (perfect correlation) for reference. The number of samples used is 37,000.

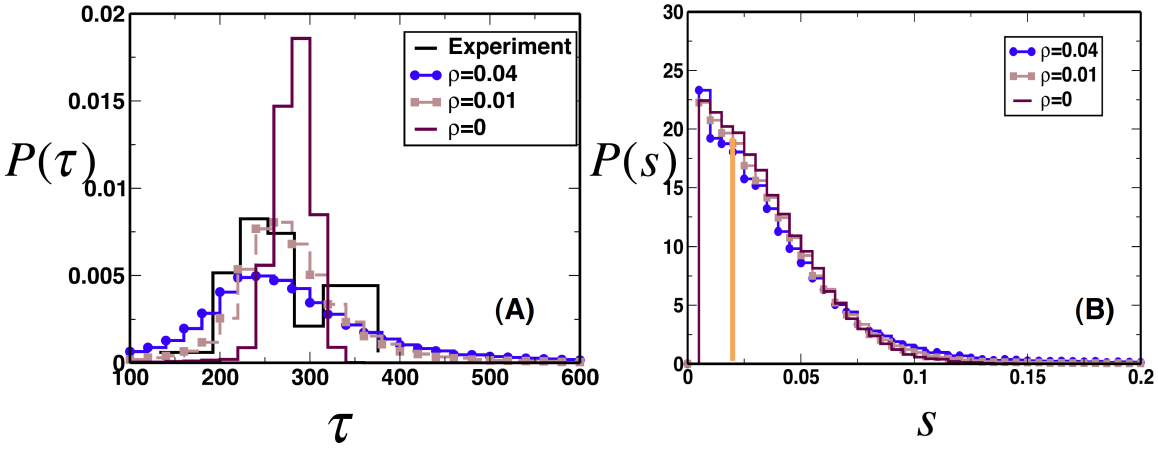

Fig S10: Comparison of the distribution of the adaptation time and precision of adaptation when the covariances are constrained as shown in Eq. (S16) for different values of ρ. (A) Adaptation time distribution for the Gaussian distribution generated by constraining the covariances between the pairs: (Tar-CheA, CheA-CheY, CheY-CheR, CheR-CheB, and CheB-CheZ), as well as the variances and the mean values of the protein abundances (**Chain Interaction**) for two different values of ρ=0.04 (blue) and ρ=0.01 (brown). We also show the case (solid Maroon) when the constrained covariances and variances were taken from the C matrix in Eq. (S17) where ρ=0 (perfect correlation) for reference. The experimental distribution is shown in black. **(B)** The distribution of the precision of adaptation for the cases as shown in (A) using the same color scheme. The orange bar indiciates the cell population average value of the precision of adaptation. The number of samples is 37,000.

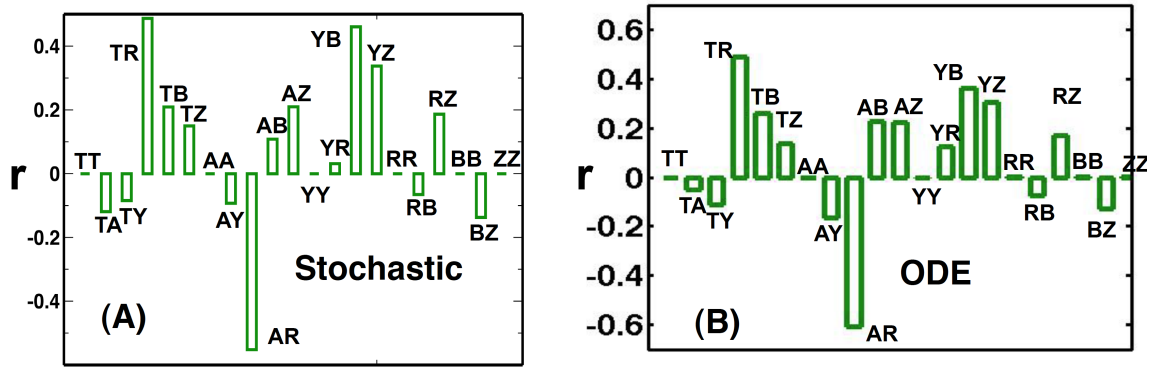

Fig S11: The effect of intrinsic noise fluctuations on the Pearson correlations between protein pairs. We constrained mean values of τ, τ^2, s, p, and, p^2 to the respective values measured in experiments, i.e., $\overline{\tau} = 245$ s, $\overline{\tau^2} = 62323.5$ s^2, $\overline{s} = 0.02$, $\overline{p} = 20\%$, and p^2= 425 and calculate **(A)** Pearson correlations $r = r_{MaxEnt} - r_{uni}$ among

protein pairs using Gillespie algorithm. **(B)** Same as **(A)** but stimulated using ODEs. The number of samples in each case is 70,000. The data is for MBL model.

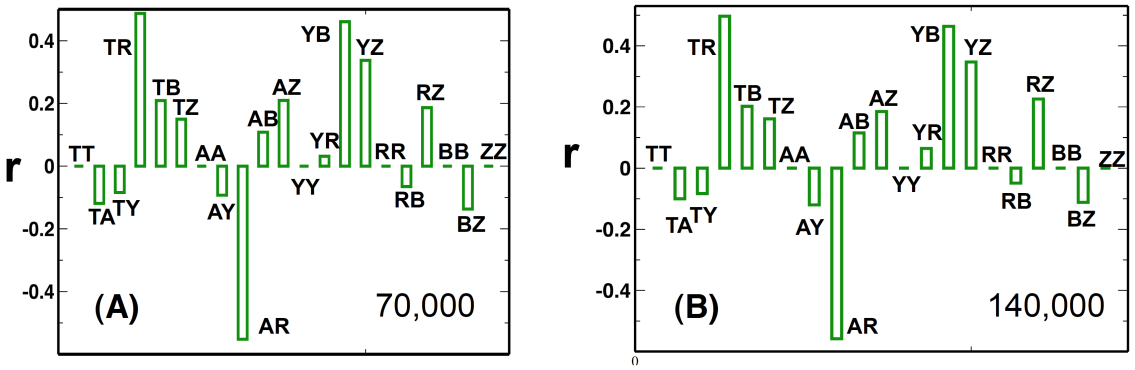

Fig S12: Convergence of the Pearson correlations for MBL model. (A) The Pearson correlations are calculated using a sample size of 70,000. **(B)** Same calculation as (A) but done with a sample size of 140,000.

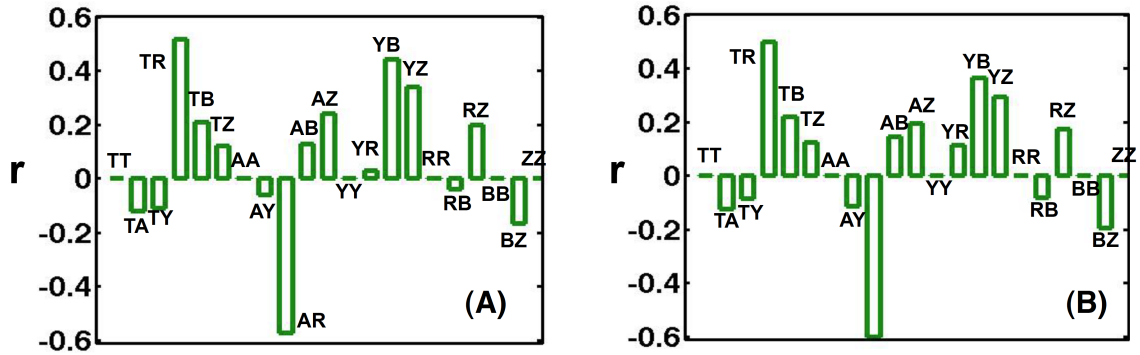

$\bar{\tau} = 245$ s, $\overline{\tau^2} = 62323$ s^2, $\bar{p} = 20$
$\overline{p^2} = 425$, $\bar{s} = 0.02$, $\overline{s^2} = 0.0005$

$\bar{\tau} = 263$ s, $\overline{\tau^2} = 71528$ s^2, $\bar{p} = 25$
$\overline{p^2} = 725$, $\bar{s} = 0.04$, $\overline{s^2} = 0.0018$

Fig S13: Sensitivity of the Pearson correlations on the values of the constraints chosen. (A) The Pearson correlations $r = r_{MaxEnt} - r_{uni}$ are calculated for different protein pairs using the MaxEnt distribution for MBL model. The values of the constraints are shown in the plot. **(B)** Same as (A), but for a different set of values for the constraints. The values used are shown in the plot. The number of samples in each case is 70,000. The data is for MBL model.

1. Kollmann M, Lovdok L, Bartholome K, Timmer J, & Sourjik V (2005) Design principles of a bacterial signalling network. *Nature* 438(7067):504-507.
2. Barkai N & Leibler S (1997) Robustness in simple biochemical networks. *Nature* 387(6636):913-917.
3. Hauri DC & Ross J (1995) A model of excitation and adaptation in bacterial chemotaxis. *Biophys J* 68(2):708-722.
4. Knox BE, Devreotes PN, Goldbeter A, & Segel LA (1986) A molecular mechanism for sensory adaptation based on ligand-induced receptor modification. *Proc Natl Acad Sci U S A* 83(8):2345-2349.
5. Alon U, Surette MG, Barkai N, & Leibler S (1999) Robustness in bacterial chemotaxis. *Nature* 397(6715):168-171.
6. Cluzel P, Surette M, & Leibler S (2000) An ultrasensitive bacterial motor revealed by monitoring signaling proteins in single cells. *Science* 287(5458):1652-1655.
7. Hlavacek WS*, et al.* (2006) Rules for modeling signal-transduction systems. *Science's STKE : signal transduction knowledge environment* 2006(344):re6.
8. Sayak Mukherjee S-CS, Veronica J. Vieland and Jayajit Das (2013) Data-driven quantification of robustness and sensitivity of cell signaling networks. arXiv:1305.3902 (Physical Biology, October 2013, in press).
9. Li M & Hazelbauer GL (2004) Cellular stoichiometry of the components of the chemotaxis signaling complex. *J Bacteriol* 186(12):3687-3694.
10. Landau LD & Lifshitz EM (1958) *Statistical physics* (Pergamon Press; Addison-Wesley Pub. Co., London, Reading, Mass.,) p 484 p.
11. Jaynes ET (1957) Information Theory and Statistical Mechanics. *Phys Rev* 106(4):620-630.
12. Jaynes ET & Bretthorst GL (2003) *Probability theory : the logic of science* (Cambridge University Press, Cambridge, UK ; New York) pp xxix, 727 p.
13. Cover TM & Thomas JA (2006) *Elements of information theory* (Wiley-Interscience, Hoboken, N.J.) 2nd Ed pp xxiii, 748 p.
14. Bialek W*, et al.* (2012) Statistical mechanics for natural flocks of birds. *Proc Natl Acad Sci U S A* 109(13):4786-4791.
15. Hamann JR & Bianchi LM (1970) Stochastic population mechanics in the relational systems formalism: Volterra-Lotka ecological dynamics. *J Theor Biol* 28(2):175-184.
16. Phillips SJ, Anderson RP, & Schapire RE (2006) Maximum entropy modeling of species geographic distributions. *Ecol Model* 190(3-4):231-259.
17. Schneidman E, Berry MJ, 2nd, Segev R, & Bialek W (2006) Weak pairwise correlations imply strongly correlated network states in a neural population. *Nature* 440(7087):1007-1012.
18. Jaynes ET (1980) The Minimum Entropy Production Principle. *Annu Rev Phys Chem* 31:579-601.

19. Presse S, Ghosh K, Lee J, & Dill KA (2013) Principles of maximum entropy and maximum caliber in statistical physics. *Rev Mod Phys* 85(3):1115-1141.
20. Kampen NGv (1992) *Stochastic processes in physics and chemistry* (North-Holland, Amsterdam ; New York) Rev. and enl. Ed pp xiv, 465 p.
21. Caticha A & Preuss R (2004) Maximum entropy and Bayesian data analysis: Entropic prior distributions. *Phys Rev E* 70(4).
22. Crooks GE (2007) Beyond Boltzmann-Gibbs statistics: maximum entropy hyperensembles out of equilibrium. *Physical review. E, Statistical, nonlinear, and soft matter physics* 75(4 Pt 1):041119.
23. Dixit PD (2013) Quantifying extrinsic noise in gene expression using the maximum entropy framework. *Biophys J* 104(12):2743-2750.
24. Elowitz MB, Levine AJ, Siggia ED, & Swain PS (2002) Stochastic gene expression in a single cell. *Science* 297(5584):1183-1186.
25. Min TL, Mears PJ, Golding I, & Chemla YR (2012) Chemotactic adaptation kinetics of individual Escherichia coli cells. *Proc Natl Acad Sci U S A* 109(25):9869-9874.
26. Lovdok L*, et al.* (2009) Role of translational coupling in robustness of bacterial chemotaxis pathway. *PLoS Biol* 7(8):e1000171.